



This is a repository copy of *Influence of switching-waveform characteristics on the performance of a single-layer-phase switched screen* .

White Rose Research Online URL for this paper:
<http://eprints.whiterose.ac.uk/805/>

Article:

Chambers, B. and Tennant, A. (2002) Influence of switching-waveform characteristics on the performance of a single-layer-phase switched screen. *IEEE Transactions on Electromagnetic Compatibility*, 44 (3). pp. 434-441. ISSN 0018-9375

<https://doi.org/10.1109/TEMC.2002.801755>

Reuse

Unless indicated otherwise, fulltext items are protected by copyright with all rights reserved. The copyright exception in section 29 of the Copyright, Designs and Patents Act 1988 allows the making of a single copy solely for the purpose of non-commercial research or private study within the limits of fair dealing. The publisher or other rights-holder may allow further reproduction and re-use of this version - refer to the White Rose Research Online record for this item. Where records identify the publisher as the copyright holder, users can verify any specific terms of use on the publisher's website.

Takedown

If you consider content in White Rose Research Online to be in breach of UK law, please notify us by emailing eprints@whiterose.ac.uk including the URL of the record and the reason for the withdrawal request.



eprints@whiterose.ac.uk
<https://eprints.whiterose.ac.uk/>

Influence of Switching-Waveform Characteristics on the Performance of a Single-Layer-Phase Switched Screen

Barry Chambers, *Senior Member, IEEE*, and Alan Tennant

Abstract—Conventional microwave-absorbing materials rely on the absorption and conversion into heat, of the electromagnetic energy incident upon them. In an alternative approach, the phase-switched screen (PSS) applies phase modulation to the reflected signal so that the energy is redistributed into sidebands with, ideally, none remaining at the original incident carrier frequency f_c . Hence, by adjusting the frequency and shape of the waveform that controls the PSS reflection coefficient, these sidebands may be positioned outside the pass-band of a receiver tuned to f_c . An investigation has been carried out to determine how the choice of control waveform and switching frequency influence the PSS performance.

Index Terms—Electromagnetic scattering, modulation.

I. INTRODUCTION

CONVENTIONAL microwave-absorbing materials operate by absorbing the electromagnetic energy incident upon them and converting it into heat [1]. In several recent papers [2]–[4], however, we have considered an alternative technique for achieving an apparent reduction in the level of the electromagnetic energy reflected from a conducting surface, using the so-called “phase-switched screen” (PSS).

In the simplest case, that of a continuous wave (CW) plane wave of frequency f_c incident on a planar PSS, the principles of operation may be explained in terms of transmission line theory. The analogue of a single-layer PSS consists of a short-circuited length, d , of transmission line with characteristic admittance Y_c and propagation constant β , across whose input terminals is placed a time-varying conductance $G(t)$. As shown in Fig. 1, $G(t)$ is defined as

$$\begin{aligned} G(t) &= G_1, & 0 < t < \tau \\ &= G_2, & \tau < t < T \end{aligned} \quad (1)$$

where T is the time period for one cycle of the waveform used to control the state of $G(t)$.

The two conductance states G_1 and G_2 , result in reflection coefficient values of ρ_1 and ρ_2 , respectively, which are defined by

$$\begin{aligned} \rho_1 &= \frac{Y_0 - G_1 + jY_c \cot \beta d}{Y_0 + G_1 - jY_c \cot \beta d} \\ \rho_2 &= \frac{Y_0 - G_2 + jY_c \cot \beta d}{Y_0 + G_2 - jY_c \cot \beta d} \end{aligned} \quad (2)$$

where Y_0 is the characteristic admittance of free-space.

Manuscript received October 22, 2001; revised March 20, 2002.

The authors are with the Department of Electronic and Electrical Engineering, University of Sheffield, Mappin Street, Sheffield, S1 3JD, U.K. (e-mail: b.chambers@sheffield.ac.uk).

Publisher Item Identifier 10.1109/TEM.2002.801755.

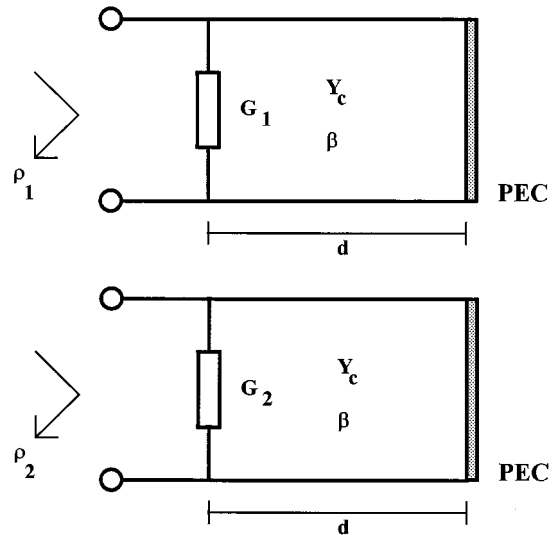


Fig. 1. Short-circuited transmission line shunted by a time-varying conductance.

Hence, a measure of the performance of the PSS as an “absorber” is the reflection coefficient Γ , when averaged over time T , i.e.

$$\Gamma = \frac{1}{T}(\tau\rho_1 + (T - \tau)\rho_2). \quad (3)$$

For no reflected signal, $\Gamma = 0$ and hence, from (3)

$$\tau\rho_1 = -(T - \tau)\rho_2. \quad (4)$$

When $d = \lambda/4$, then $\beta d = \pi/2$, and, from (2) and (4)

$$\frac{T - 2\tau}{T}(Y_0 G_1 - Y_0 G_2) + Y_0^2 = G_1 G_2. \quad (5)$$

In the simplest case, when $\tau = T/2$, then $\rho_1 = -\rho_2$ and (5) becomes

$$G_1 G_2 = Y_0^2. \quad (6)$$

In a practical PSS, the appropriate values of sheet conductance G_1 and G_2 may be obtained by switching either a layer of functional material [5] or a two-dimensional FSS array loaded with semiconductor diodes [4]. For an ideal active layer and an appropriate periodic control voltage waveform, G_1 and G_2 will approach values of 0 and ∞ and hence ρ_1 and ρ_2 will have values of +1 and -1, respectively. Thus the PSS will have a time-averaged reflection coefficient of zero and will appear to act as a perfect absorber at frequency f_c . At frequencies away from f_c ,

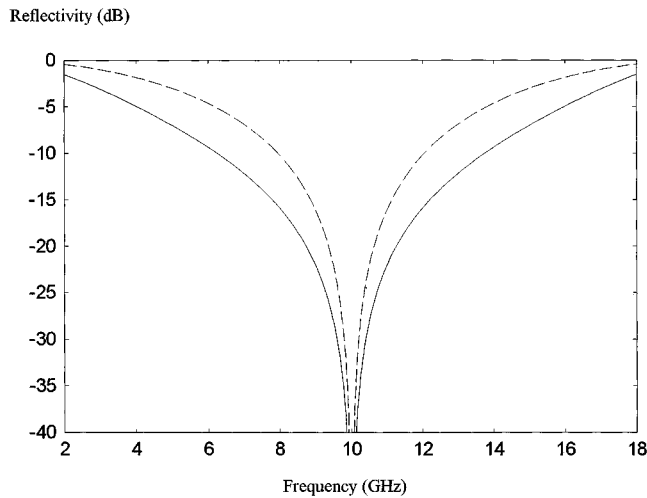


Fig. 2. Frequency characteristics of passive Salisbury screen and single-layer planar phase switched screen, $d = 7.5$ mm (— Salisbury screen, - - - PSS).

the screen thickness $d \neq \lambda/4$ and it may be shown from (2) and (3) that when $\tau = T/2$, the time-averaged reflection coefficient of the PSS is given by $\cos(\beta d)$. Hence, the PSS reflectivity, r , may be calculated from

$$r = 20 \log_{10} |\cos(\beta d)| \text{ dB.} \quad (7)$$

This is plotted in Fig. 2, for $d = 7.5$ mm, together with the corresponding curve for a conventional (i.e., passive) Salisbury screen. The reflectivity curve for the PSS has a narrower bandwidth than that of the Salisbury screen because of the absence of multiple wave reflections when $G_1 = 0, G_2 = \infty$. As G_1 and G_2 tend to Y_0 , however, the two bandwidths become identical since the PSS then reverts to a normal Salisbury screen.

Although the transmission-line model discussed above, predicts the general behavior of the PSS correctly, it does not reveal how the apparent reflectivity is dependent on the actual value of the switching frequency f_s . Also, it cannot explain what actually happens to the electromagnetic energy which is incident on the PSS. Clearly, this must all be reflected, since the instantaneous magnitude of the PSS reflection coefficient is always equal to unity. Furthermore, the model does not allow us to determine quantitatively, how the choice of switching waveform shape and frequency may be chosen, for optimum PSS performance in the presence of pulsed incident signals. In order to answer these questions, a different method of analyzing the PSS' behavior is required and that based on spectral analysis has proved to be particularly fruitful.

II. SPECTRAL ANALYSIS OF PSS FOR BIPOLAR SWITCHING

As has been noted above, at resonance, the ideal PSS presents a periodic reflection coefficient of ± 1 to an electromagnetic wave incident on its surface in such a way that the time-averaged value is zero. This is equivalent to applying binary-phase modulation to the reflected wave with the result that the energy is redistributed into sidebands with, ideally, none remaining at the original carrier frequency f_c . Hence, by adjusting the frequency of the waveform that controls the PSS reflection coefficient, these sidebands may be positioned so that they lie outside the pass-band of a receiver tuned to f_c . To illustrate this process,

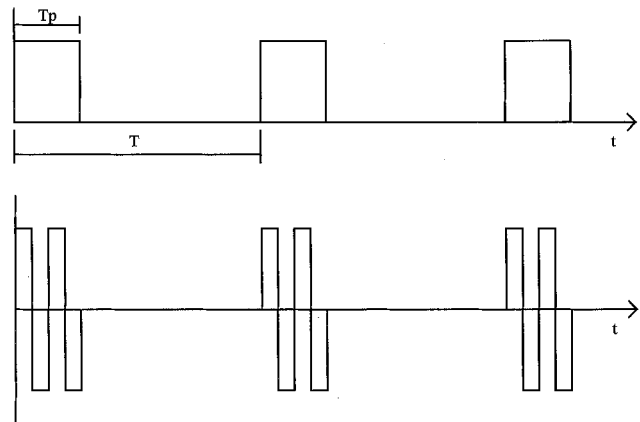


Fig. 3. Operation of the phase switched screen, (a) incident wave, (b) reflected wave ($M = 2$. For clarity, the sinusoidal carrier frequency signal itself is not shown).

consider the case of a PSS operating against a periodic train of rectangular pulses of carrier frequency f_c , as shown in Fig. 3(a). Each pulse is of length T_p and the pulse repetition period is T . After reflection from the PSS, assume that each incident carrier pulse is replaced by M cycles of a bipolar rectangular waveform, as shown in Fig. 3(b). Hence, the period of this modulating waveform, 2τ , is given by

$$2\tau = \frac{T_p}{M} \quad (8)$$

and the switching frequency, f_s , is given by $f_s = (M/T_p)$.

Since the incident pulse train is periodic, with period T , its spectrum and that of the signal reflected from the PSS may be determined using Fourier analysis. Hence, the incident and reflected signals may be written in the form

$$v(t) = \sum_{n=-\infty}^{n=+\infty} c_n e^{jn\omega_0 t} \quad (9)$$

where $\omega_0 = 2\pi/T$.

The complex Fourier coefficients, c_n , are then given by

$$c_n = \frac{1}{T} \int_0^T v(t) e^{-jn\omega_0 t} dt \quad (10)$$

For the incident periodic pulse train, c_n are given by

$$c_n = \frac{-j}{2n\pi} \left(1 - e^{-j2n\pi \frac{T_p}{T}} \right). \quad (11)$$

For the PSS-modulated wave and M integer, c_n may be written in the form

$$c_n = \frac{j}{2n\pi} \zeta \chi \sum_{m=1}^M e^{-2\gamma(m-1)} \quad (12)$$

where

$$\gamma = jn\omega_0 \tau \quad (13)$$

$$\zeta = 1 - e^{-\gamma} \quad (14)$$

$$\chi = (e^{j2\beta d} + e^{-\gamma}) \quad (15)$$

and

$$\beta = \frac{2\pi}{\lambda}. \quad (16)$$

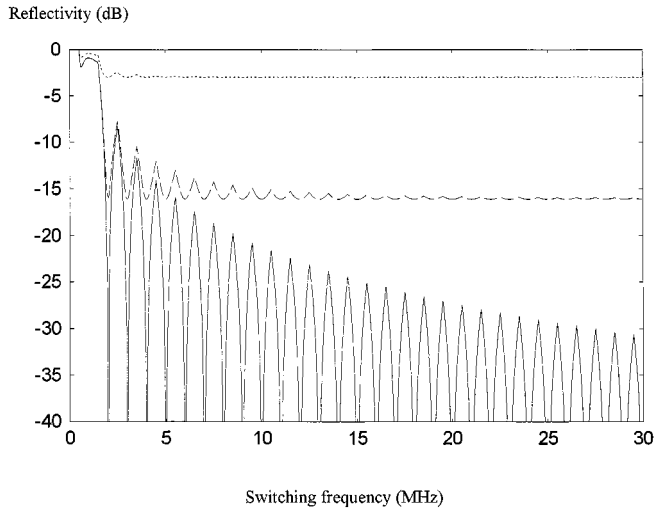


Fig. 4. Reflectivity of planar single-layer PSS with 1:1 bipolar square-wave switching ($1\text{-}\mu\text{s}$ pulse length, 100% duty cycle, i.e., CW carrier, 2-MHz receiver bandwidth) $\text{---}f_c = 10\text{ GHz}$, $\text{---}f_c = 11\text{ GHz}$, $\dots f_c = 15\text{ GHz}$.

In the general case of M noninteger, (12) is modified to

$$\text{a) } M = M + \delta M, 0 \leq \delta M \leq (1/2)$$

$$c_n = \frac{j}{2n\pi} \left[\zeta \chi \sum_{m=1}^M e^{-2(m-1)\gamma} + e^{j2\beta d} e^{-2M\gamma} \left(1 - e^{-\frac{\gamma x}{\tau}} \right) \right], \quad 0 \leq x \leq \tau. \quad (17)$$

$$\text{b) } M = M + \delta M, (1/2) \leq \delta M \leq 1$$

$$c_n = \frac{j}{2n\pi} \left[\zeta \chi \sum_{m=1}^M e^{-2(m-1)\gamma} + \zeta e^{j2\beta d} e^{-2M\gamma} + e^{-(2M+1)\gamma} \left(1 - e^{-\frac{\gamma y}{\tau}} \right) \right], \quad 0 \leq y \leq \tau. \quad (18)$$

It should be noted that (11)–(18), in the form shown above, actually give the spectral components of the incident and PSS-modulated signals relative to the carrier frequency, i.e., the component c_0 is actually at f_c .

The apparent PSS reflectivity at frequency f_c , for any switching frequency f_s , may now be found by comparing how much energy would enter the receiver pass-band in the absence of PSS modulation and when PSS modulation has taken place. In the analysis which follows, it is assumed that for a pulse-width T_p , the receiver has a total bandwidth of $2/T_p$, since this is consistent with the generally accepted rule of thumb that the receiver bandwidth at the 3-dB points is given approximately by $B = 1/T_p$.

III. BEHAVIOR OF THE PSS WITH BIPOLAR SWITCHING

Equations (11)–(18) were used initially to calculate the apparent reflectivity of a resonant (i.e., $d = \lambda/4$) PSS when the incident signal was a periodic train of $1\text{ }\mu\text{s}$ rectangular pulses of sinusoidal carrier with $f_c = 10\text{ GHz}$ and a pulse duty cycle of 100% (i.e., equivalent to the CW case). The resulting curve of reflectivity against switching frequency is shown in Fig. 4. It

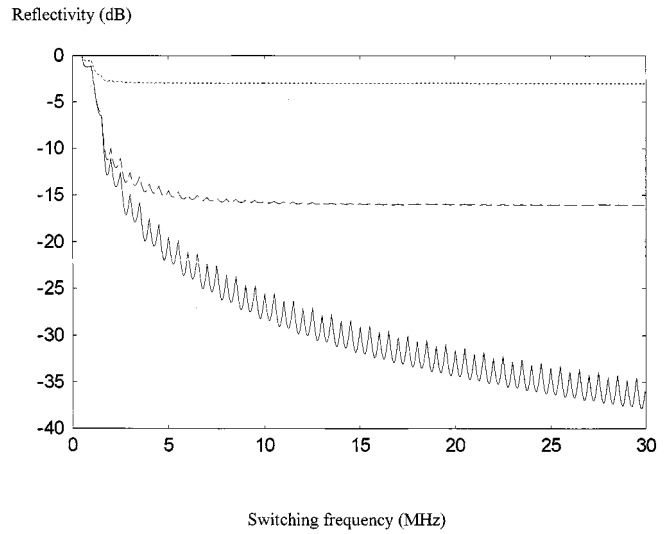


Fig. 5. Reflectivity of planar single-layer PSS with 1:1 bipolar square-wave switching ($1\text{-}\mu\text{s}$ pulse length, 10% duty cycle, 2-MHz receiver bandwidth) $\text{---}f_c = 10\text{ GHz}$, $\text{---}f_c = 11\text{ GHz}$, $\dots f_c = 15\text{ GHz}$.

Reflectivity (dB)

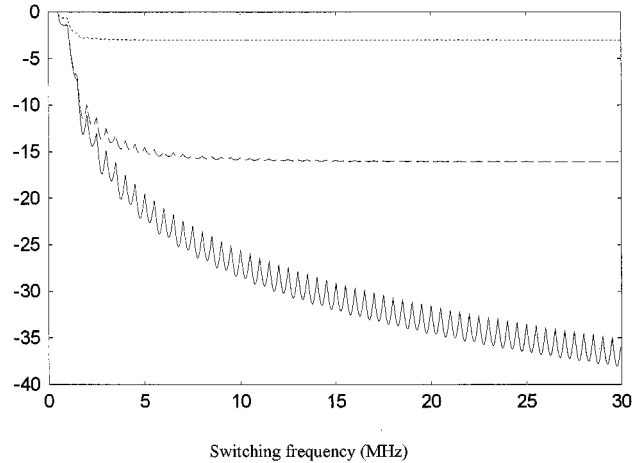


Fig. 6. Reflectivity of planar single-layer PSS with 1:1 bipolar square-wave switching ($1\text{-}\mu\text{s}$ pulse length, 1% duty cycle, 2-MHz receiver bandwidth) $\text{---}f_c = 10\text{ GHz}$, $\text{---}f_c = 11\text{ GHz}$, $\dots f_c = 15\text{ GHz}$.

can be seen that minimum reflectivity occurs when f_s is integer and this is consistent with (3) and the temporal structure of the signal reflected from the PSS, as shown in Fig. 3.

When the PSS is in a nonresonant condition ($d \neq \lambda/4$), then, it presents periodic reflection coefficients of -1 (active layer on, $G(t) = 0$) and $-e^{j2\beta d}$ (active layer off, $G(t) = \infty$) to the incident signal. The two other curves in Fig. 4 show the PSS reflectivity performance for CW incident signals at frequencies of 11 and 15 GHz. These curves are identical to those for incident signals of 9 and 5 GHz, respectively, thus confirming the symmetrical nature of the PSS frequency response. It should also be noted that for high values of switching frequency, the predicted values of PSS reflectivity agree with those calculated using (7).

The reflectivity of the PSS in the presence of pulsed incident signals is shown in Figs. 5 and 6, for pulse duty cycles of 10% and 1%, respectively. It can be seen that the PSS performance

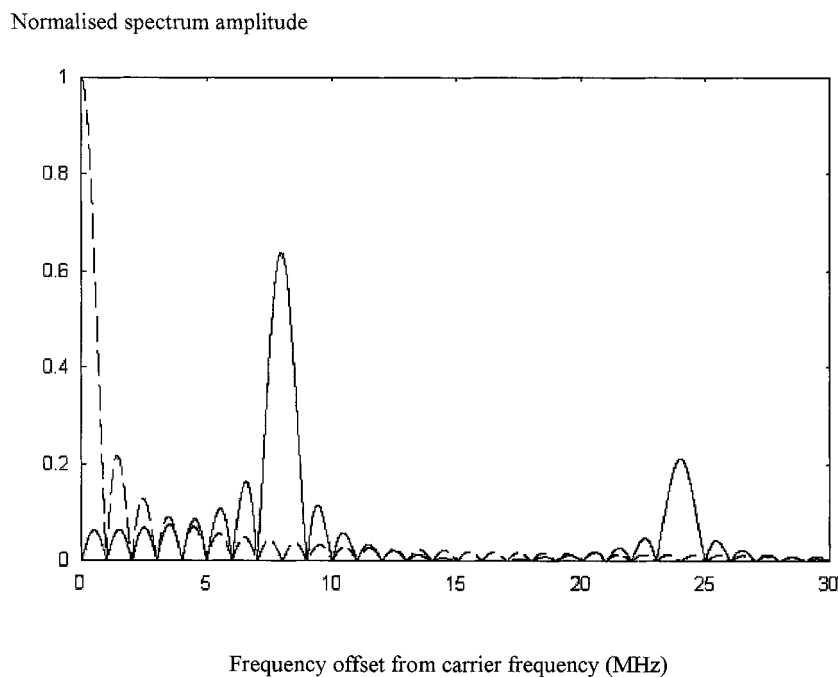


Fig. 7. One-sided frequency spectrum of pulsed carrier signal incident on and reflected from PSS switched at 8 MHz ($f_c = 10$ GHz, $1 \mu s$ pulses, 1% pulse duty cycle) (--- Incident signal, — Reflected signal).

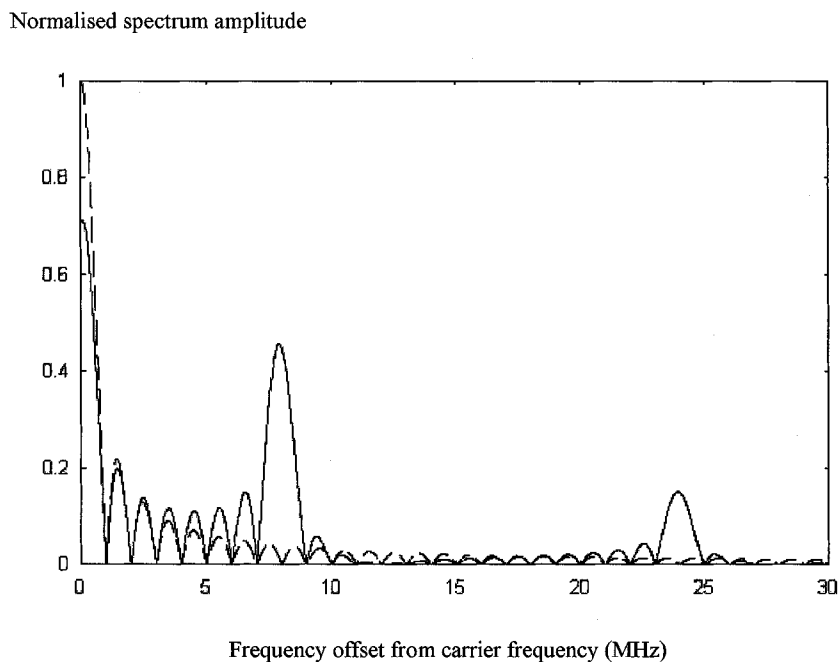


Fig. 8. One-sided frequency spectrum of pulsed carrier signal incident on and reflected from PSS switched at 8 MHz ($f_c = 15$ GHz, $1 \mu s$ pulses, 1% pulse duty cycle) (--- Incident signal, — Reflected signal).

curves for these cases follow the same trends as the CW case examined earlier. The results shown in Figs. 4 to 6 may be scaled so that they are applicable to other pulsewidths and receiver bandwidths. For example, if the pulsewidth is decreased by a factor of 10, then the receiver bandwidth and the switching frequency must be increased by the same factor to give the same value of reflectivity as before.

Consider now the spectrum of the PSS modulated signal. Fig. 7 compares the spectrum of an incident signal, composed of a train

of $1\text{-}\mu s$ pulses of carrier frequency 10 GHz and pulse duty cycle of 1%, with that of a signal reflected from a PSS whose reflection coefficient is switched between ± 1 using a 8-MHz bipolar square waveform. It can be seen that the level of the signal reflected at f_c has been reduced considerably and that the energy originally at f_c has been redistributed mainly amongst the sidebands positioned at $f_c \pm 8n$ MHz, n odd. Fig. 8 shows the corresponding spectrum when the signal incident on the same PSS is at a frequency of 15 GHz. In this case, less energy is redistributed from around f_c

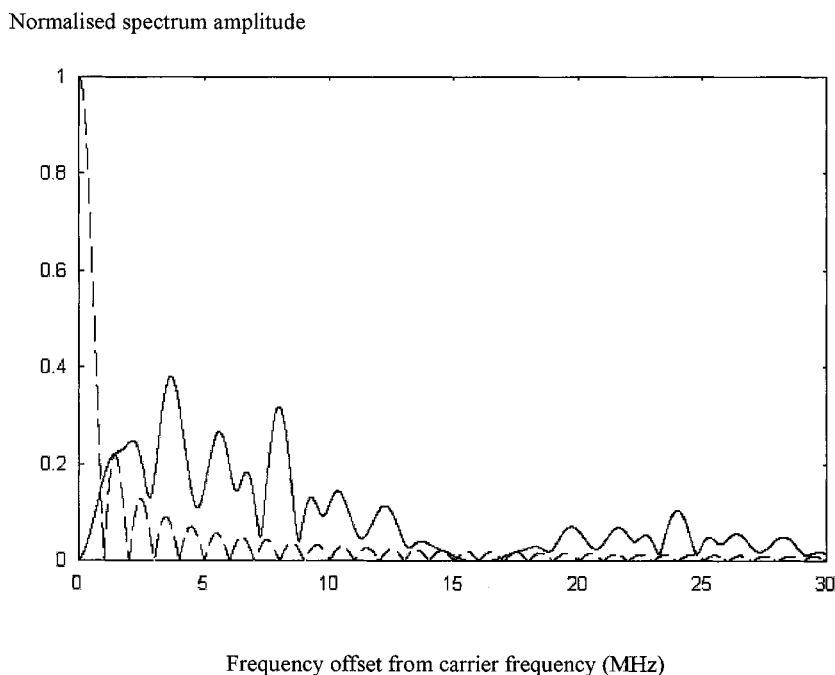


Fig. 9. One-sided frequency spectrum of pulsed carrier signal incident on and reflected from PSS switched at 8 MHz using a sequence derived from the primitive polynomial modulo 2 (4, 1, 0), $f_c = 10$ GHz, 1- μ s pulses, 1% duty cycle (--- Incident signal, — Reflected signal).

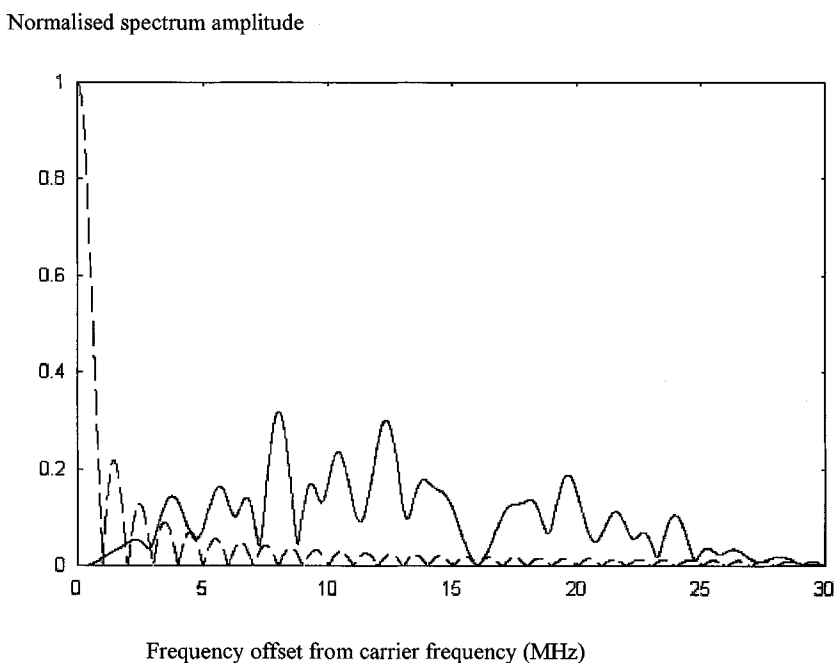


Fig. 10. As Fig. 9 but with additional Manchester encoding (--- Incident signal, — Reflected signal).

into the sidebands and so, the resulting apparent reflectivity performance is degraded from that at 10 GHz.

Returning now to Fig. 7, if the PSS was being used to reduce the apparent radar cross-section of an object, a possible countermeasure might be to periodically change the receiver bandwidth so as to detect the reflected spectral components at $f_c \pm 8$ MHz. An obvious method of avoiding this would be to increase the PSS-switching frequency, f_s , but if the PSS surface was electrically large and f_s was high enough, this might cause EMC problems or the PSS might even act as a beacon at f_s . Careful de-

sign and layout of the PSS surface should avoid these problems, but here, we look at a solution involving spectrum-spreading techniques whereby the 8-MHz sidebands are broadened out by switching the PSS reflection coefficient in a nonperiodic manner. Because such cases are not easily amenable to analytical solution using the previous Fourier analysis technique, all the results to be discussed from now on were obtained numerically using the FFT.

The sideband energy in the PSS-reflected signal may be spread out by changing the PSS-switching frequency within

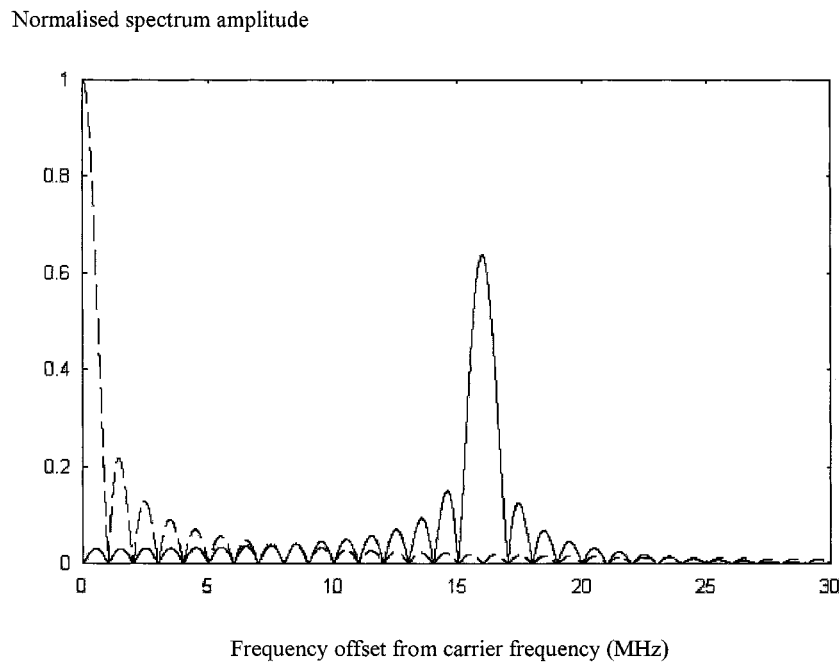


Fig. 11. One-sided frequency spectrum of pulsed carrier signal incident on and reflected from PSS with regular bipolar switching at 16 MHz. $f_c = 10$ GHz, 1 μ s pulses, 1% duty cycle (---- Incident signal, ___ Reflected signal).

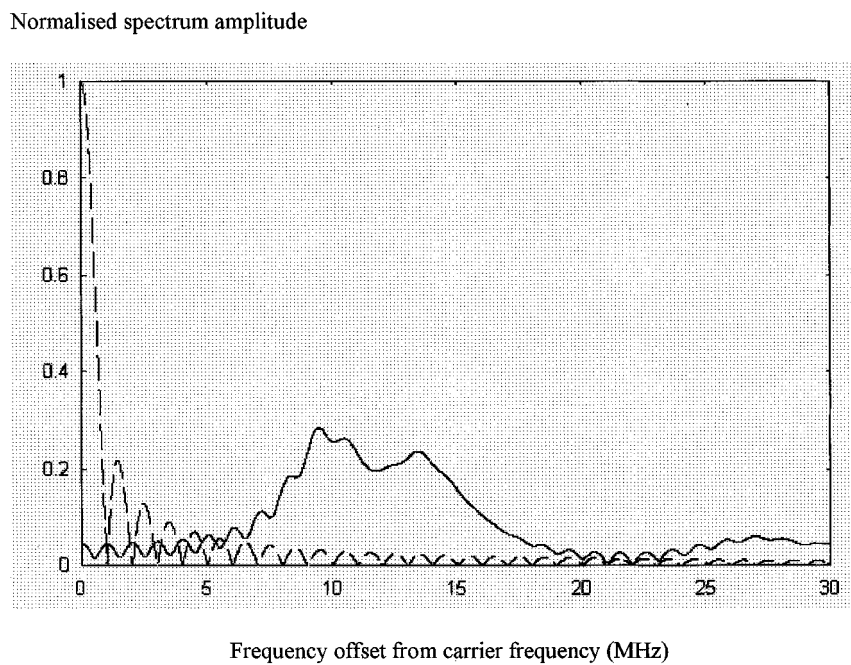


Fig. 12. One-sided frequency spectrum of pulsed carrier signal incident on and reflected from PSS with linear chirp from 8 to 16 MHz $f_c = 10$ GHz, 1 μ s pulses, 1% duty cycle (---- Incident signal, ___ Reflected signal).

the period of one radar pulse. For example, Fig. 9, shows the effect of switching using an 8-MHz bipolar waveform which has been generated using a primitive polynomial (modulo 2), of order 4 [6]. The resulting m sequence is 15 ($2^4 - 1$) b long, to which has been added an additional 0 b so as to equalize the number of ones and zeros (to ensure a zero dc level and hence zero reflected energy at f_c) and to provide the necessary 16 b (since the switching frequency of 8 MHz is equivalent to 16 half-cycles within the 1- μ s radar pulse). A further refinement is to then represent each 1 or 0 in the bit

sequence using Manchester encoding. This breaks up repeated occurrences of ones or zeros in the sequence, thus smoothing out the spectrum as well as increasing the effective switching frequency to approximately 16 MHz. The benefits of including this additional process may be seen by comparing the spectra shown in Figs. 9 and 10. If the spectrum in Fig. 10 is now compared with that obtained with regular bipolar switching at 16 MHz, as shown in Fig. 11, the superiority of the scheme using 8-MHz switching with Manchester encoding is evident. A second technique for spectrum spreading is to use a switching

TABLE I
DEPENDENCE OF PSS REFLECTIVITY ON
SWITCHING WAVEFORM CHARACTERISTICS

| PSS switching scheme | PSS Reflectivity (dB) |
|--|-----------------------|
| Periodic bipolar, 8 MHz | -23.6 |
| 4 th order polynomial, 8 MHz | -17.1 |
| 4 th order polynomial, 8 MHz with Manchester encoding | -39.0 |
| Periodic bipolar, 16 MHz | -29.7 |
| Chirped bipolar, 8 – 16 MHz | -25.7 |

waveform whose frequency is chirped during the duration of the radar pulse. Fig. 12 shows the spectrum which results when the PSS switching frequency is increased linearly from 8 MHz to 16 MHz within the 1 μ s radar pulse period. As expected, the spectral component at 8 MHz has now been spread out over the frequency range from 8 to 16 MHz, but the energy remaining within the receiver passband is still greater than in the cases of either periodic switching at 16 MHz, or switching at 8 MHz with a pseudo-random code.

A numerical comparison of the five switching schemes discussed above is given in Table I, from which can be seen the superiority of the Manchester-encoded primitive polynomial approach. Although in practice, more optimum switching strategies and higher switching frequencies would be employed, clearly the PSS shows promise for modifying the apparent real-time electromagnetic scattering characteristics of an object.

The results discussed above are idealized since the start and finish of the switching sequence and each radar pulse are synchronized and also the same switching sequence is used each time. Clearly, in practice, such synchronization cannot be obtained and because the radar receiver will almost certainly make use of pulse integration, it would be prudent to use a different switching sequence against each pulse received during the integration time so as to counter the possible use of selective time gating. The obvious way to accommodate these requirements is to use a very long switching sequence, but this must have characteristics that are not necessarily similar to those used for spread-spectrum communication systems. Most importantly, the number of ones and zeros (corresponding to the PSS reflection coefficient states of +1 and -1) in that part of the sequence which occurs for the duration of a radar pulse, whose starting and finishing times are not known *a priori*, should be identical so as to ensure minimum signal reflected from the PSS at f_c . Although this condition may often be almost met in a global sense, sequences generated using primitive polynomials, for example, are seen to be far from ideal when the local distribution of ones and zeros is examined since at some locations in the sequence there will be runs of repeated ones or zeros. Hence, the number of ones and zeros when summed over the duration of one radar pulse may differ considerably with a consequent degradation of the PSS reflectivity. This is illustrated in the top curve of Fig. 13, where the PSS is switched using a 16-b sequence which is

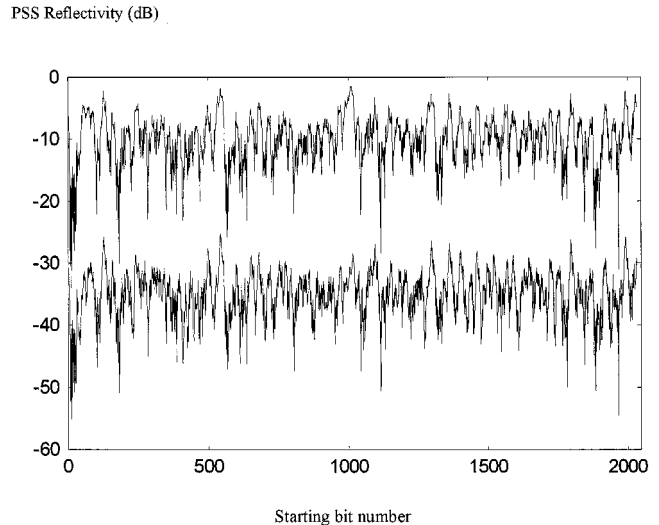


Fig. 13. Variation in PSS reflectivity as the 16-b switching sequence contained within the width of a 1- μ s radar pulse is chosen sequentially from an overall switching sequence of 2048 b. Top curve = bipolar switching based directly on the bit sequence generated by an 11th-order polynomial (modulo 2). Mean reflectivity value = -10.2 dB. Bottom curve = as top curve, but when Manchester encoding is used. Mean reflectivity value = -35.1 dB.

chosen sequentially from a 2048-b sequence generated from a primitive polynomial of order 11. The bottom curve shown in Fig. 13 illustrates how the use of Manchester encoding can improve the PSS reflectivity considerably. In this case, even though the numbers of ones and zeros in the length of the switching sequence contained within the time for one radar pulse are now identical, the PSS reflectivity is not zero since the calculation is being made over a 2-MHz receiver bandwidth rather than just at f_c . The required PSS-switching sequences also differ from those used in spread-spectrum communication systems in a second respect, namely that they should not have good autocorrelation properties so as to guard against sequence recovery, and hence, the application of electronic counter measures in the receiver.

IV. CONCLUSION

In this paper, we have discussed the concept of the PSS, which is an active technique for modifying the apparent real-time electromagnetic scattering characteristics of an object. In particular, we have investigated the influence of switching frequency and waveform characteristics on PSS performance against pulsed incident signals and identified some desirable features of switching waveform design. In practice, the behavior of real PSS structures will differ somewhat from that of the idealized continuous layers discussed above because of the presence of periodic circuit elements, bias lines, and diode packages which comprise the PSS; nevertheless our experimental work to date broadly confirms the efficacy of the technique. The discussion in this paper has been limited to the case of the single-layer PSS; theoretical and experimental studies have shown, however, that multilayer PSS have the additional advantage of frequency agility and the temporal and spectral analysis of these systems will be reported elsewhere.

REFERENCES

- [1] E. F. Knott, J. F. Schaeffer, and M. T. Tuley, *Radar Cross Section*. Norwood, MA: Artech House, 1993.
- [2] A. Tennant, "Reflection properties of a phase modulating planar screen," *Electron. Lett.*, vol. 33, no. 21, pp. 1768–1769, 1997.
- [3] B. Chambers, "Characteristics of modulated planar absorbers," *Electron. Lett.*, vol. 33, no. 24, pp. 2073–2074, 1997.
- [4] A. Tennant and B. Chambers, "Experimental phase modulating planar screen," *Electron. Lett.*, vol. 34, no. 11, pp. 1143–1144, 1998.
- [5] A. Barnes, K. L. Ford, P. V. Wright, B. Chambers, C. D. Smith, D. A. Thompson, and F. Pavri, "Materials and techniques for controllable microwave surfaces," in *Proc. 5th Eur. Conf. Smart Structures, Materials*, 2000, pp. 109–120.
- [6] E. J. Watson, "Primitive polynomials (mod 2)," *Math. Comput.*, vol. 16, pp. 368–369, 1962.



Barry Chambers (SM'99) received the Ph.D. degree in electrical engineering from the University of Sheffield, Sheffield, U.K., in 1969.

Following a period at the University of British Columbia, Vancouver, BC, Canada, he returned to the University of Sheffield, where is now Professor of radio frequency and microwave engineering in the Department of Electronic and Electrical Engineering and Head of the Communications and Radar Research Group. His current research interests include EMC, RF and microwave metrology,

electromagnetic wave scattering and novel smart electromagnetic materials and structures for application in low observable technology, EMC shielding, and communication systems.

Dr. Chambers is a Chartered Engineer and a Fellow of the Institute for Electrical Engineers (U.K.).



Alan Tennant received the B.Eng. degree in electronic engineering and the Ph.D degree in medical physics, both from the University of Sheffield, Sheffield, U.K., in 1985, and 1992, respectively.

Between 1985 and 1986, he worked with BAe Systems, Stevenage, U.K. In 1992, he joined Defence and Evaluation Research Agency (DERA), Malvern, U.K., where he worked on phased-array antenna systems, before taking up an academic post at the University of Hull, Hull, U.K. He returned to the Department of Electronic and Electrical Engineering, University of Sheffield, in 2001, as a Senior Lecturer in the Communications and Radar Group where he is involved in research into adaptive materials for radar signature management, novel three-dimensional phased array antenna topologies, and acoustic array systems.